AF Cooperative VLC Communication Systems: Cascaded Channel Analysis

A. R. Ndjiongue*, Telex M. N. Ngatched⊛ & H. C. Ferreira*
* Department of Electrical and Electronic Engineering Science, University of Johannesburg,
P.O. Box 524, Auckland Park, 2006, Johannesburg, South Africa.
⊛ Faculty of Engineering and Applied Science, Memorial University,
St. John's, NL A1B 3X5, Canada.
Emails: {arrichard,hcferreira}@uj.ac.za,tngatched@grenfell.mun.ca

***Abstract*—Visible light communications (VLC) technology is a relatively new emerging telecommunication paradigm. It offers the opportunity to design cost-effective communication systems due to the dual use of the light sources, which are exploited as illumination devices and as communication antennas. However, this technology is mostly deployed in short-range communication applications because of the light diffusion range, which is short by nature. One good response to this dilemma is the implementation of relay-assisted cooperative communication systems. Cooperative VLC systems provide three advantages, which are an increase in the transmission range, an improvement of the detection, hence of the bit error rate (BER), and an improved lighting system. In this paper, we analyze the channel response of a single-relay indoor VLC system based on an amplify-and-forward (AF) strategy. The system takes into account the fact that the relay also receives a reflected message. Results show the influence of the room's reflection index, Lambertian index, the number of scattered rays on the overall channel response and confirms the importance of relay-assisted strategies in improving systems' reliability.**

***Index Terms*—Cascaded VLC system, amplify-and-forward strategy, relay-assisted VLC system, channel response of cooperative VLC systems.**

I. Introduction

The increased thirst for high data rate and better quality of service (QoS) has led researchers to continuously carry out research in visible light communications (VLC) technology. In general, most techniques used in VLC are borrowed from radio frequency (RF) or other optical wireless communications (OWC) technologies. Examples include orthogonal frequency division multiplexing (OFDM) with its two variants direct current (DC)-offset (DCO) and asymmetric clipped optical (ACO), and cooperative relaying strategies.

In RF technology, cooperative relaying is widely used to improve reliability [1], [2]. The performance of such systems can be improved by the introduction of selectivity feedback loops from the receiver to the relay, to avoid the relay to transmit with a low signal-to-noise ratio (SNR) and enable the receiver to communicate on its SNR [3]. In general, incremental cooperative networks outperform direct transmissions. Their performance is improved by using multiple relaying systems [4]. They perform better with the introduction of incremental selective techniques in which thresholds are imposed on relays' and receiver's SNRs. This allows the receiver to send a feedback message on its own SNR to the relay. [5]. A combination of amplify-and-forward (AF) and decode and forward (DF) with an incremental selectivity, provides better performance when compared to all the above described AF and DF strategies [3].

Relay-assisted strategies have recently been proposed for OWC and VLC [6]–[16] in particular. It is shown in [6] that relay-assisted strategies are powerful techniques to mitigate fading and transmission range shortness. This is confirmed in [7], which proposed a multi-hop relay-based maritime VLC system. The system exploits a DF strategy to extend coverage in underwater VLC environments. This is illustrated in Fig. 1. [8] investigates a scenario in which user terminals can act as relays in order to extend the coverage of a VLC-based downlink. In [9] and [10], relay-assisted VLC systems based on DCO-OFDM are proposed. They confirm that cooperative VLC systems improve the transmission gain when compared to a direct link. [11] deals with a multi-user VLC system in which other users serve as a relay. The message transits through other users to reach the destination if the source-destination link is blocked or shadowed. The same technique is proposed in [12] for an inter-vehicle system in which each vehicle can serve as a relay to forward the transmitted message. A full duplex cooperative VLC system using a loop interference cancellation method is also investigated in [13] and [14]. The gamma-gamma distribution can be exploited as done in [15] to analyze a DF strategy on free space optical (FSO) links. A practical demonstration of a cooperative VLC system is proposed in [16] where an audio signal is successfully delivered to the destination over two intermediate relay terminals. These strategies are also exploited in hybrid systems with VLC. For example, in a cascaded system involving power line communications and VLC, both AF [17]–[19] and DF strategies [20] have been proposed.

Against the above background, it is clear that relay-assisted transmissions and cooperative techniques provide a great deal of contribution in improving the system reliability. Neverthe-

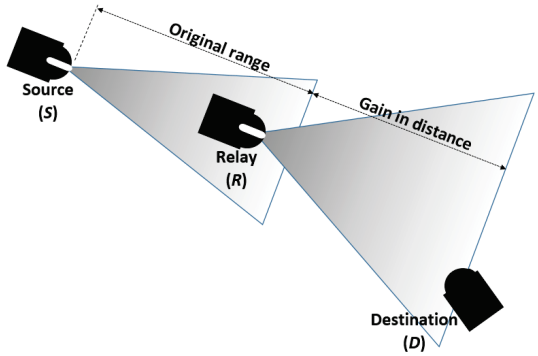

Figure 1. Illustration of improved lighting and transmission coverage due to a relay-assisted strategy. If both source and relay have the same lighting characteristics, then lighting range and transmission coverage are doubled.

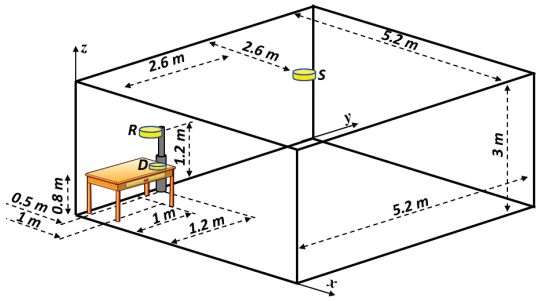

Figure 2. Transmission environment showing the light source, the relay and the main receiver.

less, many aspects of these strategies are not fully investigated in VLC technology. For example, the analysis of a single-relay VLC system in the indoor environment where the relay also receives part of the reflected message has not been fully studied. Therefore, in this paper, we analyze the indoor channel response of a single-hop VLC system, based on the AF scenario, taking into consideration the fact that relay also receives part of the reflected message.

The remainder of the paper is organized as follows: In Section II, a description of the system is given, followed by the channel model, simulation and results in Section III. Finally concluding remarks are given in Section IV.

II. Principle and System Description

A. System description

Fig. 2 illustrates a typical indoor VLC environment where a relay light is needed. The primary light source (*S*) broadcasts both light and the message from the ceiling, situated at 3 m from the floor. *S* is purposely located at the center of the ceiling of a 5.2×5.2 m^2 room. The room is a sleeping environment with a reading station equipped with a desk-light (*R*). The main light, *S*, is a sleeping light. As shown in Fig. 2, the coordinates of *R* are (0.5 m, 1.2 m, 1.2 m). *S* produces a little amount of lumens and hence, it can not be used for reading. Consequently, it is hard for the receiver, *D*, to detect the message sent by *S*. The receiver is either a smart phone with a front camera or a laptop disposed on the working table. Its coordinates are (1 m, 1 m, 0.8 m).

1) The message source (S): *S* is the main light source lighting the transmission environment. It is characterized by a Lambertian pattern of semi-angle $\Phi_{1/2}(S)$. It produces an optical power, P_t, with a luminance L_S. *S* is the antenna from which the message is originally generated.

2) The relay (R): *R* is made of two main parts: a receiving part R_R and a transmitting part R_T. R_R is a normal VLC receiver including a photo-detector (PD) and characterized by its field of view (*FoV*), FoV_R. FoV_R is wide, allowing the relay to also detect signals from reflected rays. The PD is also characterized by its responsivity λ_R. Its role is to detect the message signal from *S* and forward it to R_T for re-transmission, depending on the strategy adopted. On the other hand, R_T is normally a light source characterized by a Lambertian pattern with a semi-angle $\Phi_{1/2}(R)$. It produces an optical power, P_R, with a luminance L_R. R_T is required to forward to the main recipient the message it receives from R_R.

3) The message recipient (D): *D* is the main recipient of the message diffused by *S*. It is made of a PD, characterized by its responsivity λ_D and its wide field of view, FoV_D. It may detect signals directly from (*S*), (*R*), and reflected signals.

4) Reflecting objects: The reflecting objects over the transmission environment include walls, ceiling, floor and other object disposed over the environment. It is assumed that the relay and the message recipient receive reflected messages only from the walls. Walls are in general modeled by the Lambertian reflectance model. The reflection index of walls defines the amount of reflected rays.

B. Illumination analysis

The visible portion of the electromagnetic spectrum ranges from 380 nm to 770 nm, and represents the band of radiation perceived by the human eye. The power of light can be calculated from its energy, which is defined in quantum theory by Planck's equation. For a given light source, the relationship between irradiance and distance is defined by the inverse square law, and the falling of illuminance on a surface varies according to the Lambert's cosine law. The radiometric power of that illuminance, the luminous flux, is an important parameter related to lighting.

Most indoor VLC environments such as offices, reading rooms, kitchens, bed rooms or TV rooms are environments with illumination constraint. This implies that the amount of lumens produced by the light source must be calculated according to the lighting level required. For example, a classroom requires about 250 lumens per meter square (lm/m^2) while for a computer work, a study library or a show room, about 500 lm/m^2 are needed. To calculate these values, the knowledge of both luminous flux and illuminance are fundamental.

In regard with our system, the luminous intensity of the light from the j^{th} source, j = *S*, *R*, and walls (*W*), falling on

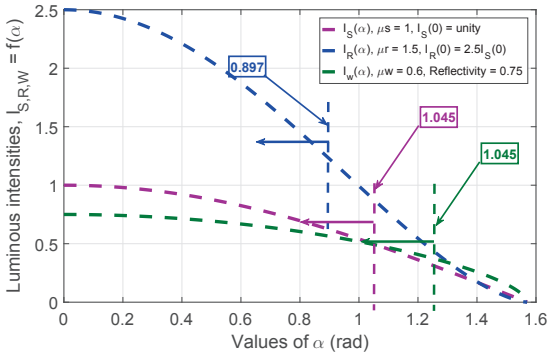

Figure 3. Luminous intensities falling on *D*, *R* and the walls.

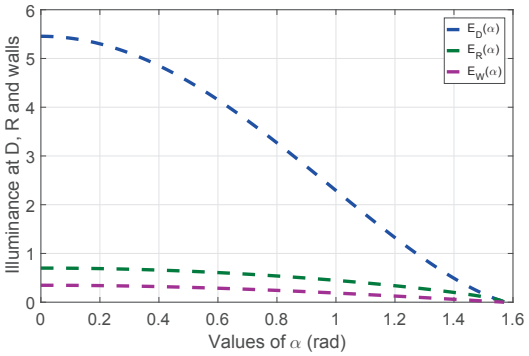

Figure 4. Illuminance at *D*, *R* and walls.

the i^{th} element, i = *W*, *D* and *R*, is given by

$$I_j = I_j(0)\cos^{\mu_j}(\alpha_i), \tag{1}$$

where $I_j(0)$ is the maximum luminous intensity produced by the j^{th} source which corresponds to the incident angle $\alpha_i = 0^o$, and μ_j is the Lambertian order of the j^{th} source. The illuminance at a point i due to the source j can be expressed as

$$E_i = \sum_{i,j}^{W,D,S,R} \frac{I_j(\alpha_i)\cos(\beta_i)}{d_i} + \varepsilon_i, \tag{2}$$

where $I_j(\alpha_i)$ is defined in Eq. (1), β_i the angle of reflection at point i, and d_i the distance from source to destination. In Fig. 3, we show the optical power intensity of *S*, *W* and *R* in terms of the emitting angle. We assume $I_R(0) = 2.5I_S(0)$. The choice of the 2.5 scaling factor is motivated by the fact that by multiplying the intensity at *S* by 2.5, the obtained value agrees with the needed reading light intensity. *S* and *R*, are given with different Lambertian orders. μ_S = 1, corresponding to $\Phi_{1/2}(S)$ = 30^o while μ_R = 1.5, corresponding to $\Phi_{1/2}(R) = 25^o$, which confers to the desk-light a more focused light beam. The walls have a Lambertian reflectivity of order, μ_W = 0.6, and a 75% reflectance coefficient. These values are chosen to match the description of the system given in Section II-A. From Fig. 3, it can be noted that the luminous intensity produced at the relay is about 2.5 times that of the main source. But the illuminance at *D* is larger than that at the relay and on the walls as shown in Fig. 4. This is because *D* receives light from *S*, *R* and *W*.

III. Channel and Model

A generalized VLC data transmission model is depicted in Fig. 5. It shows the two VLC domains and their converting equipment which are light sources in the transmitter and PDs in the receiver. A driver (D_r) is used to adapt the generated electrical current to the light source after the application of the DC-offset. Note that the signal processing block is not shown in this figure. Here, the channel includes both the filter and the noise generators while in the receiver, the block Am+F represents both the trans-impedance amplifier (TIA) and the filter. Also note that the model given in Fig. 5 represents all

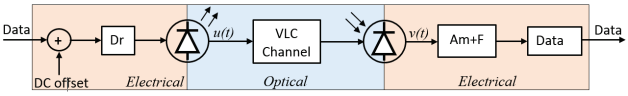

Figure 5. Generalized VLC communication model.

links (*S-D*, *S-R* and *R-D*). The TIA is used to amplify the current when it is firstly produced by the PD. Light emitting diodes (LEDs) and laser diodes (LDs), used in VLC [21], are non-coherent, hence, intensity modulation (IM) and direct detection (DD) techniques adapt well. Let $u(t)$ be the emitted optical intensity due to the light source, which follows the IM pattern. The DD function is accomplished by the photo-detector combined with a TIA. For the *S-D*, *S-R* and *R-D* links, the transmission is governed by [22]

$$v(t) = \lambda u(t) \otimes h(t) + n(t), \tag{3}$$

where $n(t)$ is the additive white Gaussian noise (AWGN). The rest of the parameters are defined as follows: $v(t)$ is the amplified output electrical current, λ the responsivity of the PD used, and $h(t)$ the channel impulse response (CIR). The CIR depends on the structure of the transmission link as it may be LoS (direct or non-direct) or non-LoS (NLoS). In the system model under consideration, the *S-D* link is made of both LoS and diffuse components. This also applies to the *S-R* link while the *R-D* link is purely LoS.

A. Channel characteristics

The CIR of these VLC links are functions of the geometry of the transmission environment and the *FoV* of the receiver. This geometry includes the position and the orientation of the light source and its LoS and NLoS properties. As a result of the above links description, the CIR is given by

$$h_\Delta(t) = h_{\Delta LoS}(t) + h_{\Delta diff}(t), \tag{4}$$

where $h_{\Delta LoS}(t)$ and $h_{\Delta diff}(t)$ are respectively the contributions of the LoS and that of the diffuse links into the CIR, and $\Delta \in \{S\text{-}D, S\text{-}R, R\text{-}D\}$. It should be noted that, $h_{\Delta diff}(t)$

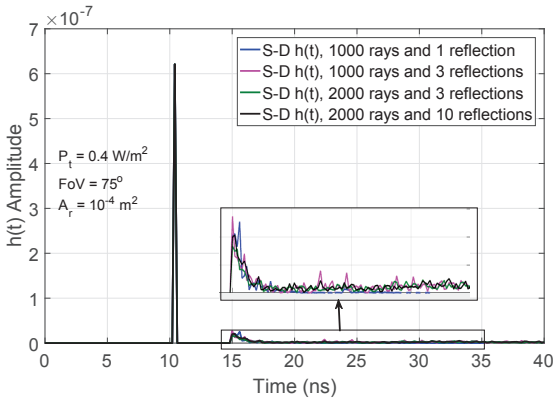

Figure 6. Channel impulse response (CIR) for the *S-D* link corresponding to four scenarios: 1000 rays - 1 reflection; 1000 rays - 3 reflections; 2000 rays - 3 reflections, and 2000 rays 10 reflections. Transmit power, P_t = 0.4 W/m^2; receiver *FoV* = 75^o and effective PD area, $A_r = 10^{-4}$ m^2.

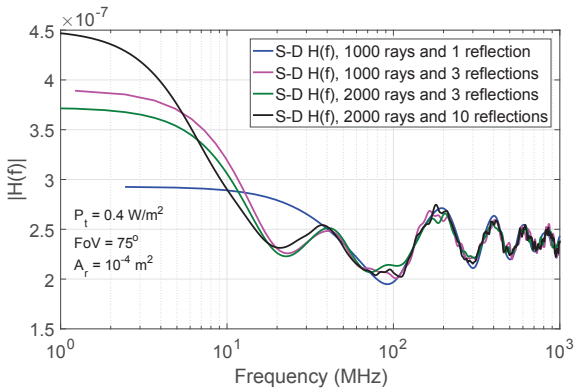

Figure 7. Channel frequency response (CFR) for the *S-D* link corresponding to four scenarios: 1000 rays - 1 reflection; 1000 rays - 3 reflections; 2000 rays - 3 reflections, and 2000 rays 10 reflections. Transmit power, P_t = 0.4 W/m^2; receiver *FoV* = 75^o and effective PD area, $A_r = 10^{-4}$ m^2.

is null for the *R-D* link since no reflection of the light emitted by the relay reaches *D*.

At the receiver i, the LoS part of the links is given by

$$h_{\Delta LoS}(t) = \sum_{j=1}^{\eta} V_j T(\alpha_i) \frac{A_r(\beta_i)}{d_i^2} \delta\Big(t - \frac{d_i}{c}\Big), \tag{5}$$

where $\eta \in \{S, R\}$, depending on the strategy adopted. In a fix strategy, the relay unconditionally always transmit and as such, is considered as a permanent antenna. In the case of incremental strategies and incremental strategies with selection based on the SNR at *D* and *R*, η = *S* when *R* is not transmitting and $\eta \in \{S, R\}$ when *R* is transmitting. We assume that the visibility function V_j is unity and that α_i and β_i may vary so that the best position is selected for all components in the system. c is the speed of light and $\delta(.)$ is the Dirac delta function. Finally, A_r is the effective receiver area and the filter function, $T(\alpha_i)$, is defined by [22]

$$T(\alpha_i) = \frac{(\mu_j + 1)\cos^{\mu_j}(\alpha_i)}{2\pi}, \tag{6}$$

where $\mu_j = \{\mu_S, \mu_R, \mu_W\}$ for the system considered.

The contribution of the NLoS links, $h_{\Delta diff}(t)$, is hard to determine as the number of reflection can not easily be calculated. This number is generally obtained by simulation [9]. $h_{\Delta diff}(t)$ depends on many factors, including and not limited to the room dimension, the reflectivity of walls, ceiling and floor, and others object disposed over the environment, and the position and the orientation of *S* and *R* [23]. If the number of reflections, *k*, is known at the receiver i, the impulse response due to light undergoing these reflections can be expressed as [23]

$$h_{\Delta diff}(t, S, R) = \frac{\mu_j + 1}{2\pi} \sum_{v=1}^{k} \rho_i \cos^{\mu j}(\alpha_i) \frac{\cos(\beta_i)}{d_i^2} \text{rect}\Big(\frac{2\beta_i}{\pi}\Big) \times h_{\Delta diff}^{v-1}\Big(t - \frac{d_i}{c}, S, R\Big) A_{ref}. \tag{7}$$

In Eq. (7), ρ_v is the reflection coefficient of the v^{th} reflector, d_i is the distance from the j^{th} source to the i^{th} reflector, A_{ref} is the area of the reflector and the quantity $h_{\Delta diff}^{v-1}\Big(t - \frac{d_{sj}}{c}, S, R\Big)$ represents the impulse response of the $(v-1)^{th}$ path. Due to the complexity of Eq. (7), the power delay profile based on the root mean square delay spread, which quantifies the properties of the multi-path link, is used. Another metric used in multi-path transmissions is the Rician factor, K, which characterizes the statistical distribution of the original message signal amplitude at the receiver. It is the ratio of the squared power of the dominant path (LoS) components to the squared power of the remaining path. Measuring K is quite difficult due to the number of path that is not easy to be determined. Nevertheless, few techniques have been proposed [24]. It is reported in [23] that K can be given as the square-ratio of the LoS frequency response by that of the diffuse link, and can be expressed as

$$K = \left[\frac{H_{\Delta LoS}}{H_{\Delta diff}}\right]^2. \tag{8}$$

Given K, the received powers, $P_{\Delta LoS}^r$ and $P_{\Delta diff}^r$, respectively due to the LoS and NLoS channels for the link Δ, are given by [23]

$$\begin{cases} P_{\Delta LoS}^r = H_{\Delta LoS} P_t & (1), \\ P_{\Delta diff}^r = H_{\Delta diff} P_t & (2), \\ P_{\Delta}^r = \big(H_{\Delta\_LoS} + H_{\Delta diff}\big) P_t & (3). \end{cases} \tag{9}$$

Based on Eq. (8), Eq. (9-3) can be rewritten as

$$P_{\Delta}^r = (1 + \sqrt{K}) H_{\Delta LoS} P_t. \tag{10}$$

B. Noise and interference scenario

Shot (Quantum), thermal (Dark current) and background radiation noises are the most important noise in the indoor

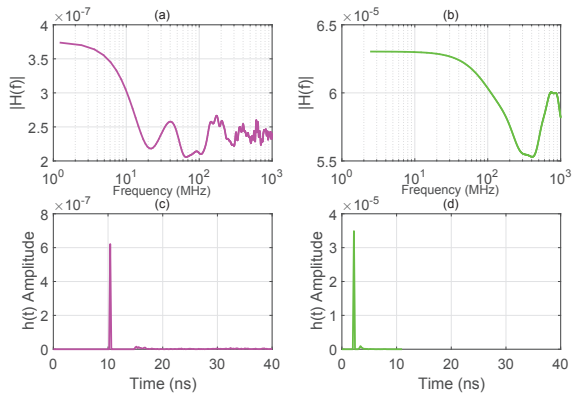

Figure 8. Channel impulse response (CIR) and channel frequency response (CFR) of both *S-R* and *R-D* links. (a): CFR of the *S-R* link; (b): CFR of the *R-D* link; (c): CIR of the *S-R* link, and d): CIR of the *R-D* link.

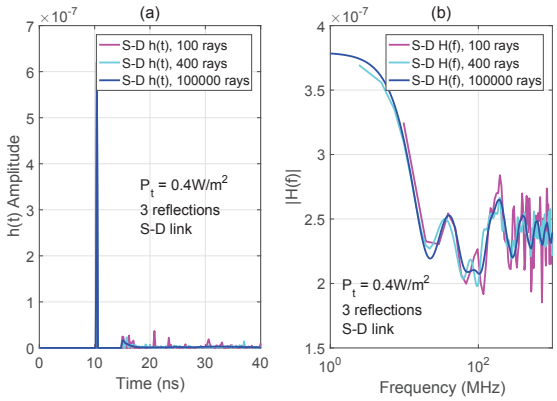

Figure 9. Channel impulse and frequency responses for the *S-D* link under the following parameters: 100, 400, and 100000 rays - 3 reflection; P_t = 0.4 W/m^2; receiver *FoV* = 75^o, and effective PD area, $A_r = 10^{-4}$ m^2.

VLC environment. Shot noise is well described by Bose-Einstein statistics when it is generated by a coherent light and is best represented by Poisson statistics if caused by a thermal light. Both distributions may exhibit a Gaussian fit for a high number of photons. Three shot noise scenarios are identified: *(i)* part of it is generated by the LoS rays from the source, *(ii)* another part is generated by the reflected light, and *(iii)* the third part emanates from the background light. On the other side, thermal noise is generated by the receiver circuitry. This happens regardless of the voltage source used to power the circuit. It is modeled using the central limit theorem (CLT), which is a normal distribution. For a high photon number, which is the case considered in this paper, shot noise is approximated to Gaussian noise. On its own side, background noise is a Gaussian white noise. Therefore, the AWGN model is used to model the channel. Note that Fano noise is also present over the environment but is generally generated with low amplitude and consequently neglected. As a result, AWGN with zero mean and variance $\sigma_n^2 = N_0/2$, N_0 being the power spectral density of the AWGN, is used.

The main interference may be generated by the light carrying the message. In fact, due to multi-path propagation, another version of the message will reach the receiver at a slightly different time. This type of interference is always present over the indoor VLC environment.

- Signal-to-noise ratio (SNR)

By substituting P_Δ^r with its expression given in Eq. (10), with a total elimination of the interference, we obtain the SNR expressed as

$$SNR = \frac{2\lambda^2 H_{\Delta LoS}(1+\sqrt{K})P_t^2}{N_0}. \quad (11)$$

C. Simulation and results

The overall simulations are based on the modified Monte Carlo Ray-tracing method [25]. The Monte Carlo method is a heuristical algorithm used to simulate system's behavior and uses random sampling to obtain results while in a Ray-tracing algorithm, the path of light is traced to generate an image.

Figs. 6 to 9 show simulation results on the characterization of an indoor VLC relay-based system. In Fig. 6, we show the CIR for the direct link between *S* and *D* for four scenarios taken randomly. Since the main source is dimmed, we assume a P_t of 0.4 W/m^2. At the destination, we assume *FoV* = 75^o and $A_r = 10^{-4}$ m^2. We vary the number of emitted rays (1000 and 2000) and the number of reflections (one, three and 10). The figure shows that the CIR produces the same first peak for the selected number of rays and reflections. The reflected signal will appear 5 ns later from the scenario with only one reflection, and the one with 10 reflections will appear the last. In Fig. 7, we show the channel frequency response (CFR) corresponding to the four scenarios of Fig. 6. The results are obtained for the same simulation parameters. The channels have the same behavior for the fours selected scenarios. The little difference is that in the case of one reflection, the first notch does not exist, which corresponds to the quick appearance of the reflected signal shown in Fig. 6. More results are depicted in Fig. 8, which presents both CIR and CFR for *S-R* and *R-D* links. The *S-R* link is depicted in Fig. 8-(a) and -(c) while the *R-D* link is given in Fig. 8-(b) and -(d). CIR and CFR for the *S-R* link are very close to the scenario, 1000 rays and 3 reflections from Fig. 6. This is due to two reasons: *(i)* The simulations are done under the same conditions (P_t of 0.4 W/m^2). At the destination, we assume *FoV* = 75^o and $A_r = 10^{-4}$ m^2, 1000 rays and 3 reflections), and *(ii) S-R* and *S-D* links have similar behaviors of their respective CIRs since *R* and *D* are physically close to each other. The *R-D* link, Fig. 8-(b) and -(d), is also simulated with P_t of 0.4 W/m^2. At the destination, we assume *FoV* = 75^o and $A_r = 10^{-4}$ m^2, 1000 rays and 1 reflection. The result shows a low attenuation of the transmitted signal. This is due to the fact that the distance from *R* to *D* is considerably

small, which implies less attenuation. The CIR in Fig. 8-(d) displays the arrival of the reflected signal with a low amplitude. Note that in terms of transmission time, the *R-D* link is faster than the *S-R* and *S-D* links. This is also related to the distance *R-D* as materialized by the first impulse which appears about 2 ns after its transmission while in *S-R* and *S-D*, the pulse arrives about 10 ns after it is sent. We show in Fig. 9 how the number of rays produced by the light source affects the channel characteristics. Recall that this number depends on the lighting pattern used, which are Lambertian or non-Lambertian. In our case, light sources have Lambertian with order μ_S = 1 ($\Phi_{1/2}(S)$ =30^o) and μ_R = 1.5 ($\Phi_{1/2}(R)$ = 25^o). This means that *S* produces more rays than *R* even though *R* gives out more power that *S*. Fig. 9 is obtained for the *S-D* link under the following parameters: $P_t = 0.4$ W/m^2, 3 reflections for 100, 400 and 100000 rays. Fig. 9-(a) shows that the number of light rays does not affect the direct link (LoS) since this is independent on the number of rays, and one ray is enough to create a LoS link. The influence of the number of rays appears when we consider the diffuse link since these rays undergo reflections. This can be observed in Fig. 9-(a). For a high number of rays, the reflected signal is more attenuated because the environment experiences a scattering of light with loss of focus. This is also explained by the reflected signal showing some significant amplitudes for a lower number of rays. In the frequency domain, Fig. 9-(b), it can be seen that within the frequency range from 0 to 20 MHz, the channel has the same behavior for the three number of rays used in the simulation. Above 20 MHz, the channel with 100000 rays is a more stabilized channel with fewer fluctuations when compared to those with a small number of rays. Note that the ringing appearing when the frequency goes beyond 100 MHz in Figs. 7, 8-(a) and 9-(b) is related to the internal characteristic of the filter that constitutes the channel.

IV. Conclusion

In this paper, we propose the channel analysis of an indoor VLC relay-assisted system using a single relay, in which the relay also receives part of the reflected signal diffused by the main source. We first analyze the illumination aspect of the environment before heading to the channel analysis. The transmission environment is a sleeping room with a working station. Based on the required illuminance at the reading surface, the main light source provides a number of lumens which is assumed to be 2.5 times lesser than that provided by the relay light. As results of the channel analysis, it is clear that the performance of a relay-assisted link is far better than that of the source-destination link. The overall transmission is affected by the number of light rays, which is related to the Lambertian order, the number of reflected rays and the reflectivity index, and finally by the position and orientation of light sources and that of VLC receivers. The analysis confirms that the performance of a relay-assisted system is improved.

References

[1] J. N. Laneman, D. N. C. Tse, and G. W. Wornell, "Cooperative diversity in wireless networks: Efficient protocols and outage behavior," *IEEE Trans. Inf. Theory*, vol. 50, no. 12, pp. 3062–3080, Dec. 2004.

[2] D. Hu and S. Mao, "Cooperative relay in cognitive radio networks: Decode-and-forward or amplify-and-forward," in *Proc. IEEE GLOBECOM Conf.*, Dec. 2010, pp. 1–5.

[3] Z. Bai, J. Jia, C. X. Wang, and D. Yuan, "Performance analysis of SNR-based incremental hybrid decode-amplify-forward cooperative relaying protocol," *IEEE Trans. Commun.*, vol. 63, no. 6, pp. 2094–2106, Jun. 2015.

[4] S. S. Ikki, M. Uysal, and M. H. Ahmed, "Performance analysis of incremental-relay-selection decode-and-forward technique," in *Proc. IEEE GLOBECOM Conf.*, Nov. 2009, pp. 1–6.

[5] M. G. Khafagy, A. Ismail, M. S. Alouini, and S. Aïssa, "Efficient cooperative protocols for full-duplex relaying over nakagami- m fading channels," *IEEE Trans. Wireless Commun.*, vol. 14, no. 6, pp. 3456–3470, Jun. 2015.

[6] M. Safari and M. Uysal, "Relay-assisted free-space optical communication," *IEEE Trans. Wireless Commun.*, vol. 7, no. 12, pp. 5441–5449, Dec. 2008.

[7] H.-J. Kim, S. V. Tiwari, and Y.-H. Chung, "Multi-hop relay-based maritime visible light communication," *Chinese Opt. Lett.*, vol. 14, no. 5, pp. 1–5, May 2016.

[8] H. Chowdhury and M. Katz, "Cooperative multihop connectivity performance in visible light communications," in *Proc. IFIP Wireless Day (WD)*, Nov. 2013, pp. 1–4.

[9] R. C. Kizilirmak, O. Narmanlioglu, and M. Uysal, "Relay-assisted OFDM-based visible light communications," *IEEE Trans. Commun.*, vol. 63, no. 10, pp. 3765–3778, Oct. 2015.

[10] R. C. Kizilirmak and M. Uysal, "Relay-assisted OFDM transmission for indoor visible light communication," in *Proc. IEEE Int. Black Sea Conf. on Commun. and Netw. (BlackSeaCom)*, May 2014, pp. 11–15.

[11] Z. Wu, *Free space optical networking with visible light: A multi-hop multi-access solution*. Boston University, 2012.

[12] C. B. Liu, B. Sadeghi, and E. W. Knightly, "Enabling vehicular visible light communication (V2LC) networks," in *Proc. 8th ACM int. Workshop on Vehicular Inter-Netw.* ACM, 2011, pp. 41–50.

[13] H. Yang and A. Pandharipande, "Full-duplex relay VLC in LED lighting linear system topology," in *Proc. 39th IEEE Annual Ind. Electron. Sty. Conf.*, Nov. 2013, pp. 6075–6080.

[14] ——, "Full-duplex relay VLC in LED lighting triangular system topology," in *Proc. IEEE Int. Symp. Commun., Control and Sig. Process. (ISCCSP)*, May 2014, pp. 85–88.

[15] M. R. Bhatnagar, "Performance analysis of decode-and-forward relaying in gamma-gamma fading channels," *IEEE Photon. Technol. Lett.*, vol. 24, no. 7, pp. 545–547, Apr. 2012.

[16] S. Jo, B. An *et al.*, "VLC based multi-hop audio data transmission system," in *Proc. Int. Conf. on Grid and Pervasive Comput.* Springer, 2013, pp. 880–885.

[17] A. R. Ndjiongue, T. Shongwe, and H. C. Ferreira, "Closed-form BER expressions for HSV-based MPSK-CSK systems," *IEEE Commun. Lett.*, vol. 21, no. 5, pp. 1023–1026, May 2017.

[18] A. R. Ndjiongue, T. Shongwe, H. C. Ferreira, T. M. Ngatched, and A. H. Vinck, "PSK to CSK mapping for hybrid systems involving the radio frequency and the visible spectrum," *Telecommun. Sys.*, vol. 64, no. 1, pp. 173–192, May 2017.

[19] A. R. Ndjiongue, H. C. Ferreira, and T. M. N. Ngatched, "Constellation design for cascaded MPSK-CSK systems," in *Proc. IEEE ICC Workshops*, May 2017, pp. 17–22.

[20] J. Song, W. Ding, F. Yang, H. Yang, B. Yu, and H. Zhang, "An indoor broadband broadcasting system based on PLC and VLC," *IEEE Trans. Broadcast.*, vol. 61, no. 2, pp. 299–308, Jun. 2015.

[21] A. R. Ndjiongue and H. C. Ferreira, "An overview of outdoor visible light communications," *Wiley Trans. Emerging Telecommun. Technol.*, vol. 29, no. 7, pp. 1–15, Jun. 2018.

[22] A. Ndjiongue, "Visible light communications (VLC) technology," *Wiley Encyclopedia of Electric. and Electron. Eng.*, pp. 1–15, Jun. 2015.

[23] Z. Ghassemlooy, W. Popoola, and S. Rajbhandari, *Optical wireless communications: System and channel modelling with Matlab ®*. CRC press, 2012.

[24] S. Mukherjee, S. S. Das, A. Chatterjee, and S. Chatterjee, "Analytical calculation of Rician K-factor for indoor wireless channel models," *IEEE Access*, vol. 5, pp. 19 194–19 212, Sep. 2017.

[25] C. M. I., W. Zhang, and M. Kavehrad, "Combined deterministic and modified Monte Carlo method for calculating impulse responses of indoor optical wireless channels," *IEEE J. Lightw. Technol.*, vol. 32, no. 18, pp. 3132–3148, Sep. 2014.